

Expression studies of the core+1 protein of the hepatitis C virus 1a in mammalian cells

The influence of the core protein and proteasomes on the intracellular levels of core+1

Niki Vassilaki, Haralabia Boleti and Penelope Mavromara

Molecular Virology Laboratory, Hellenic Pasteur Institute, Athens, Greece

Keywords

core+1 ORF; core+1/F protein; core+1/S protein; frameshift; hepatitis C

Correspondence

P. Mavromara, Molecular Virology Laboratory, Hellenic Pasteur Institute, 127 Vas. Sofias Ave, Athens 11521, Greece
Fax: +30 210 647 8877
Tel: +30 210 647 8875
E-mail: penelopm@hol.gr

(Received 20 April 2007, revised 8 June 2007, accepted 11 June 2007)

doi:10.1111/j.1742-4658.2007.05929.x

Recent studies have suggested the existence of a novel protein of hepatitis C virus (HCV) encoded by an ORF overlapping the *core* gene in the +1 frame (core+1 ORF). Two alternative translation mechanisms have been proposed for expression of the core+1 ORF of HCV-1a in cultured cells; a frameshift mechanism within codons 8–11, yielding a protein known as core+1/F, and/or translation initiation from internal codons in the core+1 ORF, yielding a shorter protein known as core+1/S. To date, the main evidence for the expression of this protein *in vivo* has been the specific humoral and cellular immune responses against the protein in HCV-infected patients, inasmuch as its detection in biopsies or the HCV infectious system remains elusive. In this study, we characterized the expression properties of the HCV-1a core+1 protein in mammalian cells in order to identify conditions that facilitate its detection. We showed that core+1/S is a very unstable protein, and that expression of the core protein in addition to proteasome activity can downregulate its intracellular levels. Also, we showed that in the Huh-7/T7 cytoplasmic expression system the core+1 ORF from the HCV-1 isolate supports the synthesis of both the core+1/S and core+1/F proteins. Finally, immunofluorescence and subcellular fractionation analyses indicated that core+1/S and core+1/F are cytoplasmic proteins with partial endoplasmic reticulum distribution in interphase cells, whereas in dividing cells they also localize to the microtubules of the mitotic spindle.

The hepatitis C virus (HCV) is a major etiological agent of chronic hepatitis, which often leads to liver cirrhosis and hepatocellular carcinoma [1–4]. A vaccine against the virus is not available at present, and therapeutic approaches are still limited [5,6]. HCV is classified into the genus Hepacivirus of the Flaviviridae family [7]. The small single-stranded, positive-sense HCV RNA genome (~9.6 kb) is flanked at both termini by conserved, highly structured nontranslated

regions and encodes a polyprotein precursor (~3000 amino acids) [8–11]. This polyprotein is co- and post-translationally processed by host and viral proteases to produce three structural (core, E1 and E2) and at least six nonstructural (NS2, NS3, NS4A, NS4B, NS5A and NS5B) proteins. Initiation of translation of the viral polyprotein is controlled by an internal ribosome entry site (IRES) located mainly within the 5'-nontranslated region of the viral RNA [12,13].

Abbreviations

core+1/F, core+1 protein expressed by translational frameshift; core+1/S, short form of core+1 protein expressed by internal translation initiation; ER, endoplasmic reticulum; β -gal, β -galactosidase; GFP, green fluorescent protein; HCV, hepatitis C virus; IRES, internal ribosome entry site; LUC, luciferase; RRL, rabbit reticulocyte lysates.

In addition, the 5'-end of the HCV polyprotein coding region encompasses a second ORF shifted to the +1 position relative to the core coding sequence. Our team was among the first to independently report that this alternative ORF produces a protein known as ARFP (for alternative reading frame protein), F (for frameshift), or core+1 (to indicate the position of the new ORF) [14–17]. Converging data from several laboratories provide evidence of the presence of specific antibodies in the sera of HCV-infected patients [14–16,18,19], as well as the presence of specific T-cell-mediated immune responses [20] suggesting that the HCV core+1 ORF is expressed during natural infection.

Expression studies have indicated that both ribosomal frameshift and internal translation initiation can lead to translation of the core+1 ORF for the HCV genotype 1a. Frameshifting is mediated by slippage of ribosomes during translation elongation at core codons 8–11 and yields a core+1 chimeric protein containing the first 8–11 amino acids of core fused to amino acids encoded by the core+1 ORF [15–17]. By contrast, internal translation initiation of core+1 can occur at the internal methionine codons 85/87, resulting in a shorter form of the core+1 protein (core+1/S) [21]. Furthermore, in the absence of codons 85/87, the core+1 codon 26 was recently found to function as an internal translation initiation site [22]. The frameshift mechanism has been extensively studied *in vitro* using rabbit reticulocyte lysates (RRL) [15–17,21,23,24]. However, despite the fact that studies have focused more on frameshifting, given that it was the first mechanism associated with core+1 expression, the data regarding this mechanism in cultured cells remain variable [15,21–24]. In contrast, internal translation initiation has been identified only in mammalian cells, and recent evidence indicates that this mechanism is the predominant mechanism associated with core+1 expression in transfected liver cells [21,22].

The biological significance of the core+1 protein remains largely unknown, as functional studies of the core+1 ORF are limited by the elusive detection of its native form in cultured cells expressing the HCV structural region or in the HCV infectious systems. In this study, we sought to characterize the expression properties and define conditions that allow detection of the HCV-1a core+1/S protein, which appears to represent the main form of core+1 expressed in transfected liver cells [21]. Transfection studies in Huh-7 cells showed that core+1/S is a very unstable protein and that its intracellular levels can be downregulated by the proteolytic activity of proteasomes. Notwithstanding

this, expression of the core protein also negatively regulates core+1/S levels. Interestingly, transfection studies in Huh-7/T7 cells supported the expression of both the core+1/S protein and the core+1 protein expressed by translational frameshift (core+1/F), suggesting that both forms of the core+1 protein can be expressed concomitantly in cultured cells under conditions that allow cytoplasmic transcription. Furthermore, analysis of the subcellular distribution of the core+1 protein by immunofluorescence and biochemical subcellular fractionation indicated that both core+1/S and core+1/F are cytoplasmic proteins, with the core+1/S protein being mainly membrane associated. Both proteins show partial endoplasmic reticulum (ER) distribution in interphase cells, and in dividing cells they also localize to the microtubules of the mitotic spindle.

Results

Intracellular levels of the HCV-1a core+1 protein in Huh-7 cells are negatively regulated by the core protein and the proteolytic activity of proteasomes

To date, several attempts to detect the core+1 protein in mammalian cells have failed, including transfection of cells with plasmid DNA encoding the core sequence or infection with recombinant herpes simplex virus expressing the core-E1–E2 sequence. Consistent with these findings, previous studies have shown that the form of the core+1 protein produced by frameshift (core+1/F), is a short-lived protein whose half-life could be substantially increased by the addition of chemical proteasome inhibitors [23,25]. Furthermore, preliminary experiments using vectors expressing chimeric core+1–luciferase (LUC) have indicated that *in cis* expression of core downregulates expression of the core+1 ORF [21]. In light of these observations, we sought to investigate expression of the core+1/S protein under conditions that prevent both core expression and the proteolytic activity of proteasomes.

To this end, we performed two series of experiments. First, a series of plasmids was constructed to allow the expression of core+1/S singly or in combination with the core protein (Fig. 1Aa). Plasmid pHPI-1494 carries the wild-type core/core+1 coding sequence, under control of the HCMV and T7 promoters. To increase protein stability, the *myc* epitope sequence (EQKLI-SEEDL) was inserted at the 3'-end of the core+1 ORF (nucleotide 825). Plasmids pHPI-1507 and pHPI-1495, which are derivatives of pHPI-1494, carry mutations that abolish the expression of core. These include

a deletion of the initiator ATG (pHPI-1507) or a deletion of nucleotides 342–514 of the core coding region (pHPI-1495). Furthermore, to increase the efficiency of core+1 expression, the *myc*-tagged core+1-coding sequence contained within nucleotides 590–825 was mutated to introduce the ATG85 initiator codon (nucleotide 598) in an optimal context for translation initiation (GCCCTCTATGG to CCGCCACCATGG) [26] (pHPI-1579, Fig. 1Ab). In addition, another plasmid was constructed, plasmid pHPI-1580, a derivative of pHPI-1579 lacking the *myc* tag sequence. Western blot analysis of Huh-7 cells transfected with the above plasmids gave the following results: the pHPI-1495 and pHPI-1507 plasmids, which failed to express core, supported the expression of a protein of ~13 kDa that was recognized by anti-(core+1) serum (anti-NK1) (Fig. 1Ba, lanes 2,4). This protein had the expected size for the core+1/S-*myc* protein and was detectable only in the presence of proteasomal inhibitors MG-132 or lactacystin (Fig. 1Bb). By contrast, no detectable levels of core+1/S-*myc* were observed from the parental pHPI-1494 plasmid, supporting the expression of the core protein even in the presence of MG-132 (Fig. 1Ba, lane 3). Core expression was monitored by western blot analysis as shown in Fig. 1Bc. As expected, introducing the initiator ATG codon 85 in an optimal Kozak context (pHPI-1579) significantly increased the levels of the 13 kDa core+1/S-*myc* product (Fig. 1C, lanes 2,4). Similarly, core+1/S-*myc* levels showed a significant increase when Huh-7 cells were treated with the proteasome inhibitor MG-132 (Fig. 1C, lanes 3,5). More importantly, a protein of ~8.5 kDa, corresponding to the untagged core+1/S protein (pHPI-1580) was produced at detectable, albeit low, levels only in the presence of MG-132 (Fig. 1C, lanes 6,7). Collectively, these results indicate that core+1/S is a very unstable protein and demonstrate that both proteasome-mediated degradation and core-protein expression account for the very low intracellular levels of the core+1/S protein in cultured cells.

The second series of experiments aimed to gain an insight into the relationship between the core and core+1/S proteins. The suppressive effect of core expression on core+1/S-*myc* levels may be due either to competition between the initiator ATG of core and the internal translation initiation codons of core+1/S for the available 40S ribosomal subunits and/or to a putative inhibitory function of the core protein on the translation or stability of the core+1/S protein. As a first step to address this question, Huh-7 cells were cotransfected with the core+1/S-*myc*-expressing plasmid (pHPI-1496) and increasing amounts of the core-expressing vector (pHPI-1499) (Fig. 2A), in the

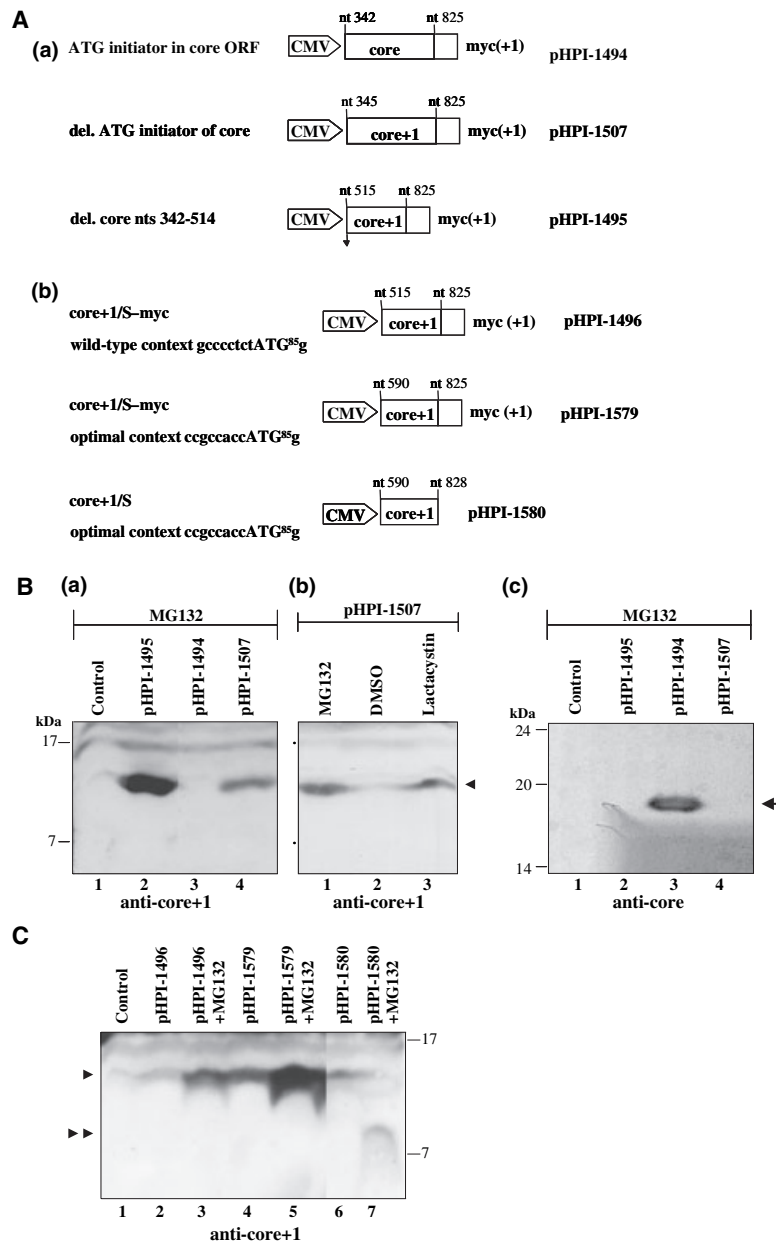
presence of MG-132. Immunoblotting indicated that core and core+1/S-*myc* were successfully expressed as proteins of the expected sizes (21 and 13 kDa, respectively) (Fig. 2B). Interestingly, the level of core+1/S was significantly reduced when coexpressed with core, in a dose-dependent manner, suggesting that the core protein exerts a negative effect on expression of the core+1 protein. To verify the specificity of the effect of core on core+1/S expression, Huh-7 cells were transfected with the vector expressing core+1/S-*myc* (pHPI-1496) and with varying amounts of a plasmid expressing an unrelated protein, β -galactosidase (β -gal), instead of core (Fig. 2A). Also, Huh-7 cells were transfected with a constant amount of β -gal-expressing plasmid, instead of the core+1/S-*myc* vector, and increasing amounts of the core-expressing plasmid. As shown by immunoblotting (Fig. 2C), the amount of core+1/S-*myc* detected was not significantly affected by the expression of β -gal. Similarly, β -gal levels remained largely unchanged when coexpressed with core (Fig. 2D). These results exclude the possibility that the decrease in core+1/S-*myc* levels in the presence of core was the result of an overloading of the cellular protein-synthesis machinery and of a shortage of its components. Finally, we examined the possible effect of core+1/S-*myc* expression on intracellular levels of core. To perform this experiment, we used the plasmid pHPI-1579 (Figs 1Ab,2A), which produces high levels of the core+1/S-*myc* protein (Fig. 1C), so that sufficient levels of core+1/S-*myc* could be detected in the presence of core, when equal amounts of the core+1/S-*myc* and core-expressing plasmids were used for cotransfection. Interestingly, the levels of core were not significantly altered by cotransfection with increasing amounts of core+1/S (Fig. 2E). Transfection efficiency in all control experiments was estimated by detecting the expression of green fluorescent protein (GFP), which is also encoded by the pA-EUA2-derived plasmids (Fig. 2B–E). Overall, these results provide strong evidence that core expression *in trans* reduces the intracellular levels of the core+1/S protein in a specific and dose-dependent manner, suggesting an effect of the core protein on the translation and/or the stability of the core+1 protein. However, no effect of the core+1 protein on core expression could be detected.

Expression of the core+1 ORF in Huh-7/T7 cells

Expression in transfected Huh-7 cells is associated with nuclear transcription, which occasionally is known to activate cryptic promoters or to be followed by post-transcriptional modifications to the newly synthesized

RNA, such as splicing [27–31] or association with nuclear proteins [29,32] which may influence its translation. Therefore, we sought to characterize core+1 expression in a mammalian expression system that could support transcription in the cytoplasm. In this case, the conditions for core+1 expression are closer to that supporting the expression of the viral RNA during natural HCV infection of the host cell. For this, we used a stable retrovirally transformed Huh-7 cell line that constitutively synthesizes the bacteriophage T7 RNA polymerase (T7 RNAP) in the cytoplasm (referred to as Huh-7/T7). The core/core+1 sequence

contained within nucleotides 342–825, followed by the *myc* epitope sequence fused to the core+1 frame, in the absence or the presence of the N6 mutation that abolishes core translation, were placed under the control of the HCV IRES element, giving rise to plasmids pHPI-1705 and pHPI-1706, respectively (Fig. 3A). The presence of the HCV IRES is important to ensure translation of the core+1 gene in Huh-7/T7 cells, inasmuch as RNA molecules transcribed in the cytoplasm remain uncapped and therefore can be translated only by a cap-independent mechanism. In the HCV IRES-containing constructs, initiation of transla-



tion is mediated by a direct binding of the 40S subunit to the AUG start codon of the polyprotein. Transfected Huh-7/T7 cells were treated with MG-132 at 12 h post transfection and harvested 24 h later, as control expression studies have shown that T7-driven LUC activity normally peaks at 24 h post transfection in this system (data not shown). As shown in Fig. 3Ba, both plasmids yielded expression of the 13 kDa *myc*-tagged core + 1/S protein, predicted to be translated by internal initiation at core + 1 codons 85/87. Surprisingly, however, both pHPI-1705 and pHPI-1706 plasmids also supported the expression of a larger form of the core + 1 protein with an apparent molecular mass of 22 kDa, which is predicted to be produced by the + 1 frameshift event at core codons 8–11 (core + 1/F). As expected, the expression levels of core + 1/S and core + 1/F yielded from pHPI-1706 were higher than those derived from pHPI-1705 (Fig. 3Ba), suggesting that core expression negatively regulates the intracellular levels of both core + 1/S and core + 1/F proteins. Core expression was tested by immunoblotting (Fig. 3Bb). To confirm that a comparable total amount of protein was analyzed for each transfectant, the amount of actin in each sample was analyzed by immunoblotting with an anti-actin rabbit polyclonal serum (Fig. 3Bc).

Because the core + 1 gene was cloned under both the HCMV and T7 promoters, we cannot exclude the possibility that core + 1/S has been produced from transcripts generated by *PoIII* at 24 h post transfection. To assure exclusively cytoplasmic transcription, we made a new construct that carries the N6 mutated IRES–core + 1–*myc* cassette under the control of the T7 promoter alone (pHPI-1748, Fig. 3A). In this case, all IRES–core + 1–*myc* transcripts and the resulting chimeric core + 1–*myc* protein molecules should be

generated exclusively by T7 RNA polymerase activity in the cytoplasm. T7-driven core + 1 expression was assessed in the presence of the N6 mutation to ensure efficient levels of core + 1/S. As shown in Fig. 3C, the data are comparable with those observed before, indicating that both core + 1/S–*myc* and core + 1/F–*myc* proteins were expressed at detectable levels from pHPI-1748.

Taken together, these data confirm the synthesis of a short form of the core + 1 protein (core + 1/S) derived from internal translation initiation at the core + 1 codons 85/87. Most importantly, our results showed that in contrast to expression in Huh-7 cells, both core + 1/F and core + 1/S proteins are synthesized in Huh-7/T7 cells, where cytoplasmic transcription is supported. Interestingly, both forms of the core + 1 protein can be expressed concomitantly under our experimental conditions. Furthermore, the suppressive effect of core protein's expression on core + 1 levels was confirmed in the Huh-7/T7 cells.

Subcellular localization of the core+1 protein

The subcellular localization of the core + 1/S protein was analyzed by immunofluorescence in Huh-7 cells transiently transfected with the *myc*-tagging vector pHPI-1579 (Fig. 1Ab) and was compared with that of the core + 1/F protein, expressed from pHPI-1509 (see Experimental procedures). As shown in Fig. 4Aa–c, part 1, the core + 1/S–*myc* protein showed partial colocalization with the ER-bound protein calnexin, in double immunofluorescence experiments using an anti-*myc* mAb for the detection of core + 1/S–*myc* and a polyclonal anti-calnexin serum for calnexin staining. In dividing cells, core + 1/S–*myc* was also found to

Fig. 1. Characterization of core+1/S–*myc* expression. (A) Schematic illustration of the *myc*-tagging constructs used in the transfection assays. (a) The *myc* epitope sequence was fused to the 3'-end of the HCV-1 core+1 ORF. The pHPI-1494 plasmid carries the intact core/core+1 sequence contained within nucleotides 342–825, whereas the plasmids pHPI-1507 and pHPI-1495 contain deleted forms of the core/core+1 sequence, lacking the initiator ATG and nucleotides 342–514, respectively. (b) The HCV-1 core/core+1 coding sequence contained within nucleotides 590–825, either *myc*-tagged at the 3'-end of the core+1 ORF (pHPI-1579) or untagged (pHPI-1580), was mutated in the context of the ATG85 initiator codon (nucleotide 598), so as to introduce an optimal Kozak context for translation initiation. The core+1/S–*myc* plasmid vector pHPI-1496 carrying the corresponding wild-type sequence is also shown. (B) Effect of proteasome inhibitors and core expression on the intracellular levels of the core+1/S protein. (a,c) Huh-7 cells were transfected with 1 $\mu\text{g}\cdot\text{well}^{-1}$ of the parental vector pcDNA3.1(-)/Myc-His B (control; lane 1) or the plasmids pHPI-1494 (lane 3); pHPI-1495 (lane 2); or pHPI-1507 (lane 4), respectively, and subsequently treated with MG-132. Cell lysates were analyzed by western blotting with the anti-(core+1) serum (a) or anti-core mAb (c). (b) Huh-7 cells transfected with the plasmid pHPI-1507 and treated with MG-132 (lane 1); dimethylsulfoxide (the solvent of MG-132; lane 2); or lactacystin (lane 3). Proteins were visualized by western blotting with the anti-(core+1) serum. The core+1/S–*myc* and core proteins are indicated with a filled arrowhead and an arrow, respectively. The migration positions of the molecular mass markers are shown on the left. (C) Optimization of the translation initiation of the core+1/S protein at codon ATG85. Huh-7 cells transfected, as described above, with the plasmids pHPI-1496 (lanes 2, 3); pHPI-1579 (lanes 4, 5); pHPI-1580 (lanes 6, 7) or the parental vector pA-EUA2 (control, lane 1) were treated with MG-132 (lanes 1, 3, 5, 7) or left untreated (lanes 2, 4, 6). Expression of the *myc*-tagged (lanes 2–5) or untagged (lanes 6, 7) core+1/S protein was detected by western blotting with the anti-(core+1) serum. The single and double filled arrowheads indicate the *myc*-tagged and untagged core+1/S proteins, respectively. The migration positions of molecular mass markers are shown on the right.

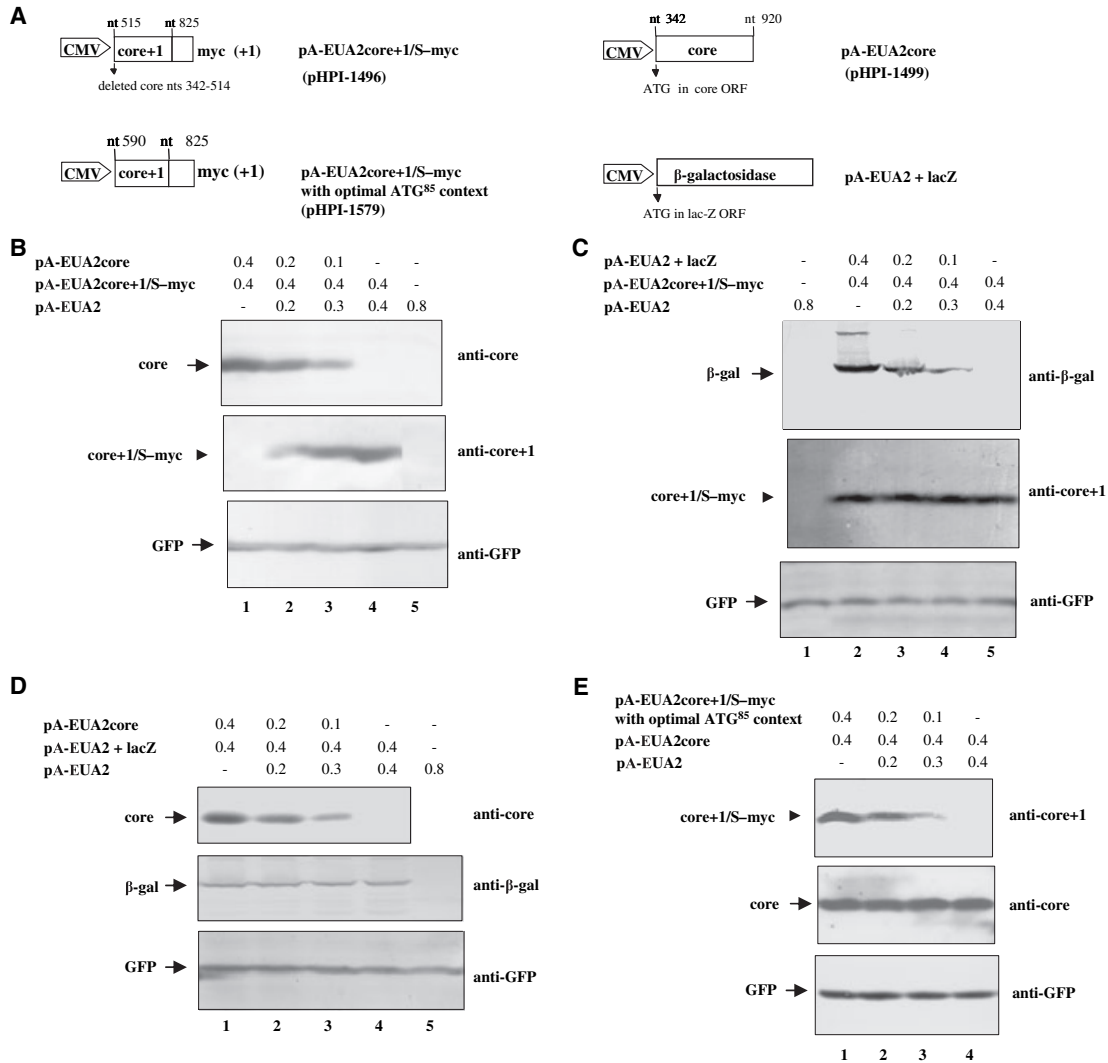


Fig. 2. Suppression of intracellular HCV core+1/S levels upon HCV core coexpression in mammalian cells. (A) Schematic representation of the constructs used in cotransfection experiments, carrying the DNA sequences encoding the HCV-1 core+1/S-myc with the wild-type (pHPI-1496) or optimal (pHPI-1579) ATG85 context, the full-length HCV-1 core (pHPI-1499), or the β -gal (pA-EUA2 + lacZ) protein. (B) Dose-dependent effect of core on the intracellular levels of the core+1/S protein. Cotransfection of Huh-7 cells using the pHPI-1496 plasmid ($0.4 \mu\text{g}\cdot\text{well}^{-1}$) together with various amounts of the pHPI-1499 (0.1, 0.2 or $0.4 \mu\text{g}\cdot\text{well}^{-1}$). The quantity of transfected DNA was kept constant ($0.8 \mu\text{g DNA}\cdot\text{well}^{-1}$) by the addition of the parental plasmid pA-EUA2. The quantity of DNA used for transfection is indicated in micrograms above each lane. Western blotting was performed to visualize the core+1/S-myc and core proteins, using anti-(core+1) serum and anti-core mAb, respectively. Transfection efficiency was estimated by assessing the expression of GFP as an internal control from the pA-EUA2 derived plasmids. (C, D) Control experiments to assess the specificity of the core inhibitory effect on core+1/S. Huh-7 cells were cotransfected with the core+1/S-myc-expressing vector (pHPI-1496) and various quantities of a pA-EUA2 derived vector expressing an unrelated protein, β -gal in the place of core (C), or with various amounts of the core expressing vector (pHPI-1499) and the β -gal-expressing vector in the place of core+1/S-myc (D), as described above. The core+1/S-myc, core, β -gal and GFP proteins were detected by western blotting. (E) Effect of core+1/S protein on core. Huh-7 cells were cotransfected with DNA encoding the core protein and increasing quantities of the core+1/S-myc-expressing vector pHPI-1579, as described above. In the cotransfection experiments depicted in (B), (C) and (E), where the core+1/S-myc vector was used, cells were treated with MG-132. The filled arrowheads indicate the core+1/S-myc fusion protein. The proteins core, β -gal and GFP are indicated by arrows.

colocalize with the mitotic spindle microtubules at different phases of mitosis, by double immunolabeling with anti-myc mAb and polyclonal anti-(α -tubulin) serum (Fig. 4Ad-f, part 1). Partial colocalization of

core+1/S-myc with microtubules was also detected in interphase cells (Fig. 4Ag-i, part 1) by double immunolabeling with the anti-(core+1) serum and an anti-(α tubulin) mAb. In addition, the protein was detected

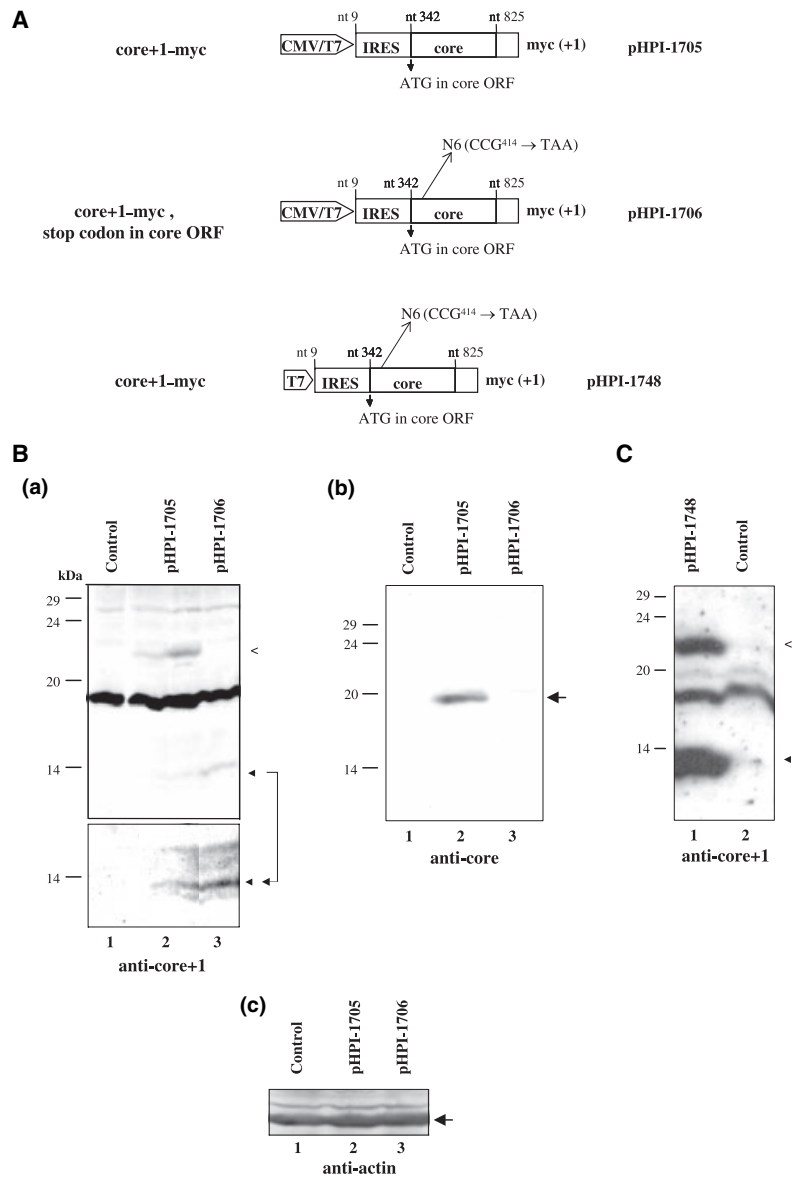
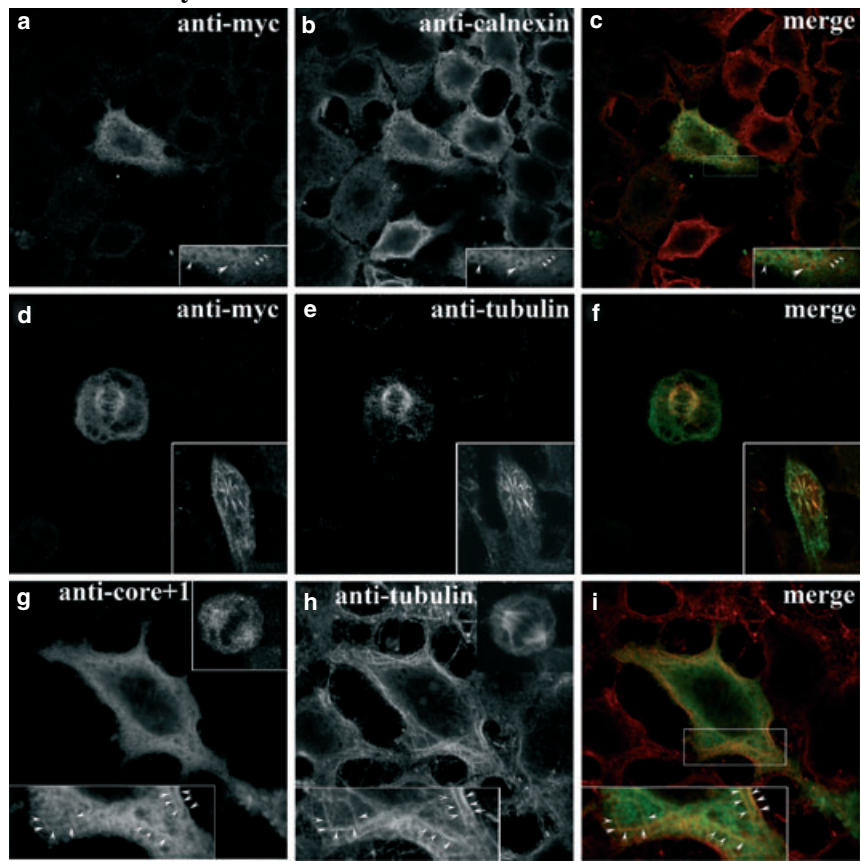


Fig. 3. Detection of both *myc*-tagged core+1/F and core+1/S proteins in transiently transfected Huh-7/T7 cells. (A) Schematic representation of the *myc* fusion constructs used in the transfection assays. The *myc* epitope sequence was fused to the 3'-end of the HCV-1 core+1 ORF. Plasmid pHPI-1705 carries the wild-type HCV-1 IRES-core/core+1 sequence (nucleotides 9–825), whereas plasmid pHPI-1706 contains a mutated variant of this sequence harboring the N6 nonsense mutation, designed to abolish core translation, under the control of both the HCMV and T7 promoters. Plasmid pHPI-1748 carries the HCV-1 IRES-core/core+1 sequence (nucleotides 9–825) under the control of the T7 promoter alone. (B, C) Huh-7/T7 cells (10^6 in B and 2×10^7 in C) were transiently transfected, as described in the legend to Fig. 1B, either with the parental vector pcDNA3.1(-)/Myc-His B (control; B lane 1, C lane 2) or with the plasmid pHPI-1705 (B lane 2), pHPI-1706 (B lane 3) or pHPI-1748 (C lane 1) and treated with MG-132. Cell lysates were analyzed by western blotting with anti-(core+1) serum (Ba,C) or anti-core mAb (Bb). The lower panel in (Ba) represents a longer exposure of the bottom part of the blot that is directly above. To confirm that a total amount of protein was analyzed in each condition, actin was detected by immunoblotting (Bc). The migration profiles of core+1/F–*myc* and core+1/S–*myc* proteins, at ~22 and 13 kDa, respectively, are indicated by the open and filled arrowheads. The arrows show core and actin. The migration positions of molecular mass markers are shown on the left.

in the periphery of the cell (Fig. 4Ad–f and g,h insets, part 1). Notably, despite the small size of core+1/S,

no protein was detected in the nucleus [33–35], suggesting that it is tightly bound to cell components in the cytoplasm. Similar results were obtained for the core+1/F–*myc* protein, in colocalization studies with

A1. core+1/S-myc



A2. core+1/F-myc

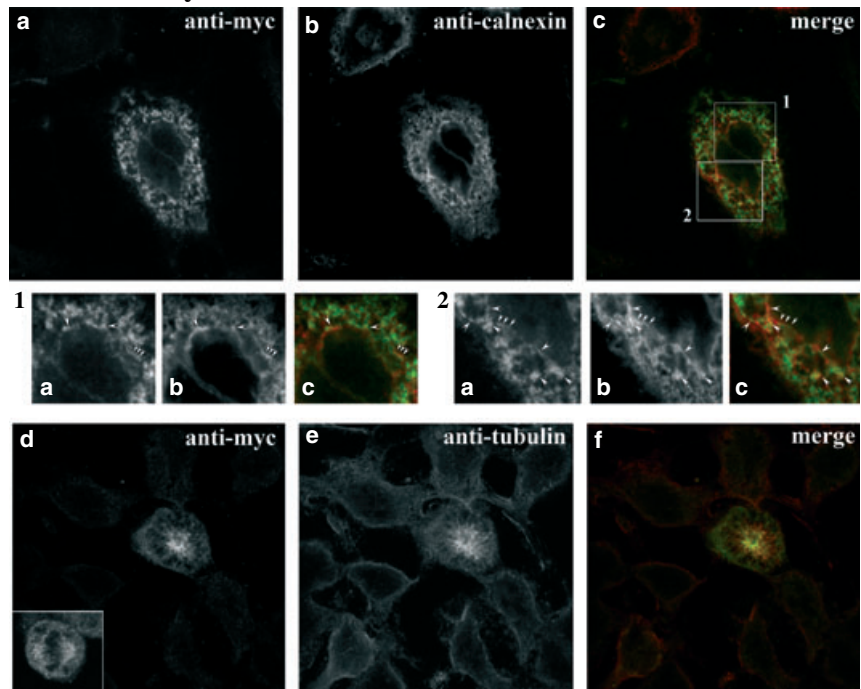


Fig. 4.

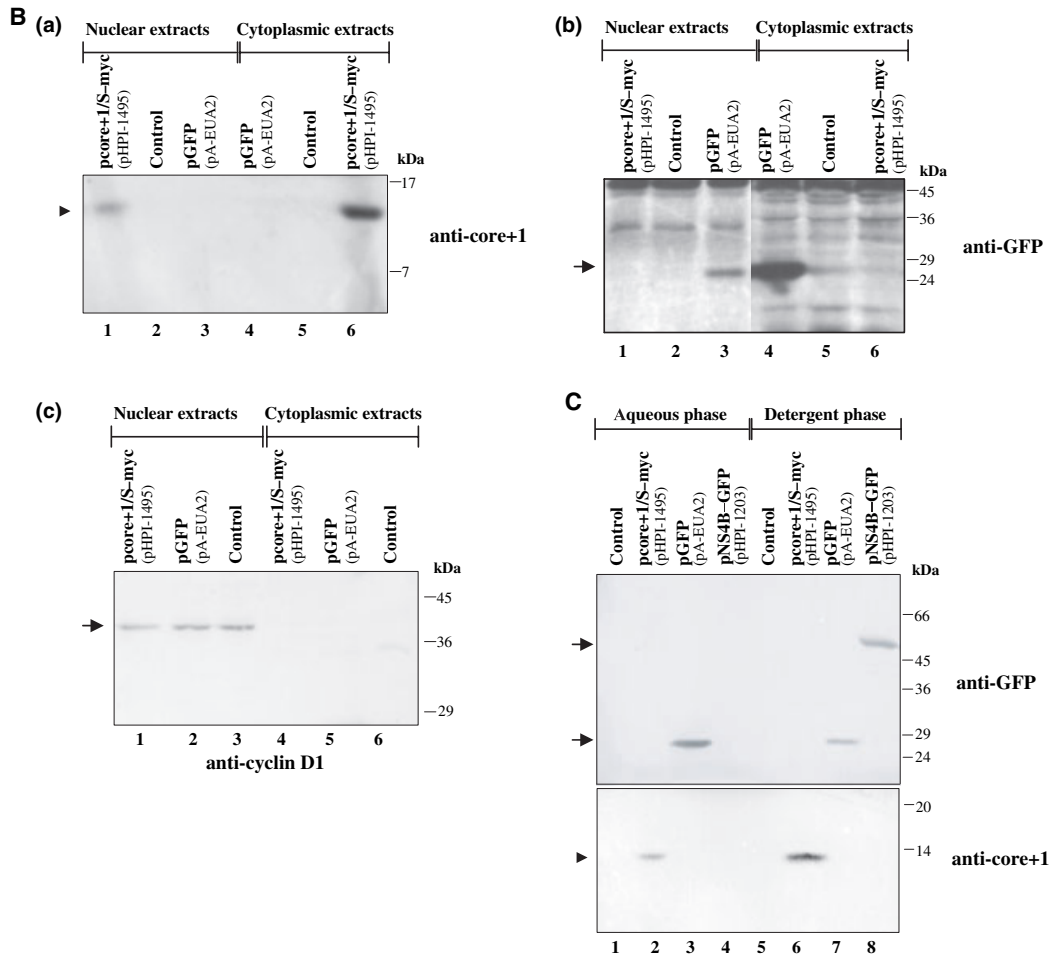


Fig. 4. Subcellular localization of core+1 protein. (A) Analysis by confocal fluorescence microscopy. Huh-7 cells cultured on 10-mm coverslips were transfected with the vector expressing core+1/S-myc (pHPI-1579) (A1) or core+1/F-myc (pHPI-1509) (A2). Transfected cells were treated with MG-132 and processed for immunolabeling (see Experimental procedures). For core+1/S-myc or core+1/F-myc localization, anti-myc mAb and Alexa Fluor 546-conjugated goat anti-(mouse IgG) were used. For core+1/S-myc localization, polyclonal anti-(core+1) serum and Alexa Fluor 647-conjugated goat anti-(rabbit IgG) were used as well. The ER marker calnexin was detected with the polyclonal anti-calnexin and Alexa Fluor 647-conjugated goat anti-(rabbit IgG) α -Tubulin was detected using polyclonal anti-(α -tubulin) and Alexa Fluor 647-conjugated goat anti-(rabbit IgG) in the case of anti-myc and anti-(α -tubulin) double labeling, or with anti-(α -tubulin) mAb and Alexa Fluor 546-conjugated goat anti-(mouse IgG) in the case of anti-(core+1) and anti-(α -tubulin) double labeling. Black and white images on the left and middle panels correspond to labeling of each protein. The merged images for the double immunolabelings are shown as colored images on the right panels (merge). The green pseudocolor represents Alexa 546 fluorescence in (A1c,f) and (A2c,f) or Alexa 647 fluorescence in (A1i). The red pseudocolor represents Alexa 647 fluorescence in (A1c,f) and (A2c,f) and Alexa 546 fluorescence in (A1i). (A1a–c,g–i) The panels to the lower right (A1a–c) and lower left (A1g–i) corners represent $\times 2$ magnifications of the framed area. The panels to the lower-right corners of (A1d–f) and upper-right corners of (A1g,h) show cells at different phases of mitosis. (A2a–c) Details 1 and 2 shown as small panels at the bottom are $\times 2$ magnifications of the framed areas in (A2c). (A2d) The framed panel at the lower left corner shows a cell in mitosis. Arrowheads in the magnified details indicate points of colocalization. (B) Fractionation of nuclear and cytoplasmic fractions. Separation of cytoplasmic and nuclear fractions from lysates of Huh-7 cells transfected with the core+1/S-myc expressing plasmid pHPI-1495 and treated with MG-132, and their analysis by western blotting using anti-(core+1) serum (a). Lysates from cells transfected with the GFP-expressing vector pA-EUA2 (a, b, lanes 3,4) or from untransfected cells (a, b, lanes 2,5) were also analysed by western blotting using with anti-GFP (b) and anti-actin (c) serum. (C) Triton X-114 phase-separation assay. Cells expressing the core+1/S-myc protein after transfection with the plasmid pHPI-1495 were treated with MG-132. Cell lysates were mixed with Triton X-114 and subjected to detergent phase separation (see Experimental procedures). Aliquots of the aqueous (lane 2) and detergent (lane 6) phases were analyzed by western blotting with anti-(core+1) serum. GFP (lanes 3, 7) and NS4B-GFP (lanes 4, 8) contained in the lysates of Huh-7 cells transfected with the corresponding expression vectors pA-EUA2 and pHPI-1203, were used as positive controls and were detected with anti-GFP serum. The aqueous and detergent phases separated from lysates of untransfected Huh-7 cells (treated with MG132) were used as negative controls (lanes 1 and 5). The core+1/S-myc protein is indicated by the filled arrowhead. Arrows indicate the positions of the GFP, NS4B-GFP and cyclin D1 proteins. The migration positions of molecular mass markers are shown on the right.

calnexin (Fig. 4Aa–c, part 2) or α -tubulin (Fig. 4Ad–f, part 2). The specificity of the antibodies was analyzed in control untransfected (NT) Huh-7 cells (data not shown).

To confirm the data obtained by immunofluorescence for the subcellular distribution of the core+1/S protein, biochemical cell fractionation was performed in transfected cells. Crude cell fractionation of Huh-7 cells transfected with the core+1/S-*myc*-encoding vector pHPI-1495 (Fig. 1Aa) into cytoplasmic and nuclear extracts and subsequent western blot analysis indicated that core+1/S was recovered mainly in the cytoplasmic fraction (Fig. 4Ba, lanes 1,6). GFP, expressed by pA-EUA2, was recovered in both cytoplasmic and nuclear extracts (Fig. 4Bb, lanes 3,4). Untransfected Huh-7 cells were used as the negative control (Fig. 4Ba,b, lanes 2,5). The efficiency of the fractionation assay to clearly separate cytoplasmic from nuclear extracts was evaluated by analyzing the distribution of cyclin D1 in the nuclear fraction (Fig. 4Bc, lanes 1–6). Interestingly, when membrane proteins were separated from soluble proteins by the Triton X-114 phase-separation assay [36], the core+1/S-*myc* protein expressed in Huh-7 cells was predominately recovered in the detergent phase as a membrane-associated protein (Fig. 4C, lanes 2,6). A small amount, $\sim 15\%$, of the core+1/S-*myc* protein was detected in the aqueous phase. The chimeric NS4B-GFP and GFP proteins expressed in Huh-7 cells transfected with the corresponding pEGFP-N3/NS4B (pHPI-1203) and pA-EUA2 plasmids were detected after the same phase separation assay, either mainly in the detergent or in the aqueous phase, respectively, as expected by their membrane-bound or soluble nature (Fig. 4C, lanes 4,8 and 3,7). Analysis of lysates from untransfected Huh-7 cells (used as negative controls) by the same assay confirmed the specificity of the anti-(core+1) and anti-GFP sera (Fig. 4C, lanes 1,5).

Overall, the above data indicated that the *myc*-tagged forms of the core+1/S and core+1/F proteins are cytoplasmic and show partial ER distribution in transfected mammalian cells. The core+1/S protein appears to associate mainly with cellular membranes. Interestingly, core+1/S and core+1/F were also found to colocalize with microtubules during mitosis, a colocalization also detected in interphase cells, although to a lesser extent.

Discussion

Expression of a novel HCV protein, encoded by an ORF overlapping the core coding sequence in the +1 frame, has recently been documented by studies

conducted in several laboratories [37]. However, functional studies on this protein have been limited by the fact that its detection in mammalian cells and in the HCV infectious system is elusive.

This study shows that intracellular levels of the core+1 protein in mammalian cells are strongly influenced not only by proteasome activity, but also by expression of the core protein. A *myc*-tagged form of the core+1/S protein was detectable only in the presence of proteasome inhibitors and in the absence of core expression, indicating that, like the core+1/F protein [23,25], the short form of core+1 is also a very unstable protein. Consistent with our results, both core+1/F and core+1/S proteins are predicted to be unstable proteins using the PROTPARAM tool (<http://expasy.org/tools/protparam.html>), which predicts the instability of a protein on the basis of the presence of certain dipeptides the occurrence of which is significantly different in the unstable proteins compared with those in the stable ones [38]. The instability indexes predicted for the core+1/F and core+1/S proteins are 45.63 and 51.91, respectively.

Interestingly, the existence of a relationship between core and *myc*-tagged core+1/S was shown when core was introduced either *in cis* or *in trans*, suggesting that the attenuating effect of core on core+1/S expression may not be limited to competition between translation initiation events, but may also be exerted at the post-translational level. Whether or not HCV core induces proteasome-mediated core+1 degradation remains an open question. However, growing evidence points to a targeting of proteasomal activity by a diverse range of viral proteins as part of a strategy for efficient virus propagation [39–45]. In fact, it was recently reported that the core protein of HBV stimulates the proteasome-mediated degradation of the HBV X protein (HBX), when the HBV viral proteins, which are transcriptionally transactivated by the X protein, reach a level sufficient for viral replication [46–50]. Furthermore, the HCV core protein was shown to interact directly with the activator of the interferon- γ inducible immunoproteasome PA28 γ as a means of regulating the nuclear retention and stability of core [51]. Collectively, these data support the hypothesis that the inhibitory effect of core on core+1/S may be part of a feedback mechanism that may be exerted through a core-mediated enhancement of proteasome activity that is specific for the core+1 protein. Certainly the possibility exists that the suppressive effect of core on core+1 expression levels may be mediated by alternative mechanism(s).

Interestingly, these findings correlate with data showing that tumors of HCV patients are likely to

accumulate the core+1 protein [37], while the levels of core are greatly reduced [52]. Although immunohistochemical studies on core+1 are not yet available, the possibility that core+1 levels are increased in HCC is supported by studies showing the accumulation of mutations in HCV RNA sequences in a number of patients with HCC and their association with increased expression of core+1 in cell-free systems [53–59]. Furthermore, a relatively high prevalence of anti-(core+1) sera has been found in patients with HCC [18,60].

Importantly, we have shown for the first time that Huh-7/T7 cells support the synthesis of both the core+1/S and core+1/F proteins from the HCV-1a isolate [1]. Possible differences in the RNA structure of the gene or in RNA–protein interactions that may underlie nuclear versus cytoplasmic transcription may explain the significant difference observed in frameshift efficiencies between the Huh-7 and Huh-7/T7 expression systems. However, the internal translation initiation events at codons 85/87 were functional in both expression systems with no significant differences. The concomitant expression of core+1/S and core+1/F proteins in Huh-7/T7 cells suggests that expression of these two proteins is not mutually exclusive at the level of translation.

The subcellular distribution of the *myc*-tagged core+1/S protein in transfected mammalian cells was studied in comparison with that of core+1/F. Both *myc*-tagged core+1/S and core+1/F proteins were found to be cytoplasmic despite their small size, which would justify passive diffusion through nuclear pores [33–35]. More specifically, both proteins showed partial colocalization with the ER and were also detected at the cell periphery. Notably, the core+1/S protein was primarily associated with membranes. Association of the core+1 protein with membranes cannot be justified by the presence of a transmembrane domain, inasmuch as no significant or only a marginally significant probability was predicted for the presence of transmembrane helices within the core+1 sequences, including the two predicted hydrophobic regions at amino acids 29–45 and 95–118 [TMPRED (<http://www.ch.embnet.org>), TMHMM (<http://www.cbs.dtu.dk>), HMMTOP (<http://www.enzim.hu/hmmtop/>) [61,62], http://npsa-pbil.ibcp.fr/cgi-bin/npsa_automat.pl?page=/NPSA/npsa_sopm.html]. The functional importance of core+1 association with the ER membranes merits further investigation, as the ER represents the localization site for most HCV proteins and of the HCV replication complex [63–65]. Furthermore, a possible interaction of the core+1 protein with the mitotic spindle and microtubules, as suggested by our immunofluorescence data, is intriguing and points to a number of

potential functions for the core+1 protein with regard to the regulation of microtubule dynamics and mitosis.

The biological role of the core+1 protein(s) and their possible contribution to some of the known functions of the overlapping HCV core remain largely unknown. It is of interest to mention that the average percentage identity of the core+1 amino acid sequence is significantly lower than that of the overlapping core protein but very close to that of E1 and NS2 proteins [66]. Furthermore, using the BLAST (<http://www.ncbi.nlm.nih.gov/BLAST/>, <http://dove.embl-heidelberg.de/Blast2/>) as well as the SSEARCH, we searched for regions of local similarity between the core+1 protein sequence and sequences of SwissProt database. In agreement with previous reports [15], we observed no clear sequence homologies between core+1 and other proteins of known function. However, we found a statistically important homology (45% identity over 44 residues length alignment) [67] between core+1 fragment amino acids 72–115 and the transmembrane domain of the ATP-binding cassette transporter subfamily A (ABCA1) amino acids 27–69. The *ABCA1* (*ABCI*) gene product translocates intracellular cholesterol and phospholipids out of macrophages and genetic aberrations in *ABCA1* cause perturbations in lipoprotein metabolism [68]. Any putative implication of core+1 in lipid metabolism would be intriguing inasmuch as HCV replication is associated with the modulation of multiple genes involved in lipid metabolism [69].

The location of the core+1 ORF within the viral genome, the findings that the core+1 ORF can be expressed independently of the polyprotein synthesis, in combination with the short half-life of the core+1/S protein due to its proteasome-mediated degradation and to its downregulation by the core protein, favor a regulatory function for this protein in the viral life cycle. It is now well established that HCV [70–72], like several other viruses (HIV-1, TMV and TYMV plant viruses) [73–75], make use of the proteasome-mediated degradation pathway for efficient viral replication, escape from host innate immunity, or inhibition of cellular apoptosis.

Also, in support of a regulatory role for core+1 in cell viability and viral persistence, earlier studies have shown that a nonstructural protein is encoded by the N-terminal structural region of a number of positive-sense RNA viruses, such as the N^{pro} protease in classical swine fever virus (CSFV) pestivirus [76], the L (leader) protease in foot-and-mouth disease virus (FMDV) (aphthovirus, picornavirus) [77], and the L* protein in Theiler's murine encephalomyelitis virus (TMEV) (cardiovirus, picornavirus) [78].

To date, we have been unable to detect the core+1 protein in the *in vitro* infectious system. Although more experiments are in progress, the possibility is open that core+1 expression may not be favored during the productive stage of the viral life cycle. This is also supported by the finding that core expression negatively regulates the intracellular levels of core+1. Studies addressing whether core+1 expression is involved in HCV persistence and/or the development of HCC through evasion of host immune responses or controlling cell growth, await the development of the appropriate experimental models. Nevertheless, the transfection systems currently in use can provide the first valuable information concerning the nature and function of HCV proteins, as many such results have been confirmed in infectious systems.

Experimental procedures

Chemicals

The proteasome inhibitors MG132 (Z-Leu-Leu-Leu-CHO) and lactacystin were purchased from Affinity Research Products (Exeter, UK) and used within the indicated times at concentrations of 5 and 25 μM , respectively. The protease inhibitor cocktail for mammalian extracts (containing AEBSF, aprotinin, leupeptin, bestatin, pepstatin a and E-64) was obtained from Sigma (St. Louis, MO).

Plasmid construction and site-directed mutagenesis

Cloning was performed following standard protocols [79]. Site-directed mutagenesis was carried out using the QuikchangeTM kit (Stratagene, La Jolla, CA). Mutations were confirmed by sequencing. The basic characteristics of the different plasmids used in this study are summarized in Table 1.

Myc-tagging constructs

All the *myc*-tagging constructs carry the *myc* epitope sequence fused to the 3'-end of the HCV-1 [1] core+1 ORF, at nucleotides 825. Plasmid pHPI-1494 contains the HCV-1 core/core+1 sequence between the initiator ATG codon of the polyprotein (nucleotide 342) and the 3'-end of the core+1 ORF (nucleotide 825). The corresponding sequence was amplified by Vent DNA polymerase (New England Biolabs, Ipswich, MA, USA) in PCR using as template the plasmid pHPI-755 [16], which contains nucleotides 342–920 of the HCV-1 core/core+1 sequence, and the primer pair C53–C203 (Table 2). First, the C53–C203 PCR product was digested with *EcoRI* and inserted into the *EcoRI* cloning site of pcDNA3.1(-)/Myc-His B (Invitrogen,

Madison, WI) to yield pHPI-1494. Plasmids pHPI-1507 and pHPI-1495 contain deleted forms of the HCV-1 core/core+1 sequence, lacking the initiator ATG and nucleotides 342–514, respectively. Deletion of the initiator ATG was performed by site-directed mutagenesis using as template pHPI-1494 and the primer pair N294–N295 (Table 2). The core/core+1 sequence between nucleotides 342 and 514 was deleted by excision of the *XhoI* fragment of pHPI-1494. Plasmids pHPI-1705 and pHPI-1706 were constructed by inserting the *XhoI*–*XhoI* fragment of pHPI-1429 and pHPI-1453, respectively, carrying the IRES-core/core+1 sequence (nucleotides 9–514) in the absence or presence of the N6 mutation [21], respectively, into the *XhoI* site of pHPI-1495. Plasmid pHPI-1429 contains nucleotides 9–825 of the HCV-1 IRES-core/core+1 sequence fused to the GFP gene in the core+1 frame and was constructed by two-step cloning. First, pHPI-790 was derived by insertion of the IRES-core(nt 9–630)-LUC sequence of pHPI-768 [16], after *HindIII*–*SalI* digestion, into the *HindIII* and *SalI* cloning sites of pEGFP-N3 (Clontech, Mountain View, CA, USA). Second, the *KpnI* fragment of pHPI-790, containing nucleotides 585–630 of the core/core+1 sequence followed by the LUC gene, was replaced with the *KpnI* fragment containing nucleotides 585–825 of the core/core+1 sequence derived from pHPI-1428. Plasmid pHPI-1428 contains the HCV-1 core+1 coding sequence from nucleotide 385 to nucleotide 825, fused to the GFP gene in the +1 frame. pHPI-1453 was constructed by inserting mutation N6 [21] into pHPI-1429 to change the 25th codon (CCG, Pro25) of the core ORF (at nucleotide 414) to a TAA stop codon. Plasmid pHPI-1509 was constructed by site-directed mutagenesis using as template pHPI-1494 and the primer pair N246–N247 (Table 2), which deleted an A residue from core codons 8–11. In all the above constructs, the core+1–*myc* cassette is under the control of the HCMV and T7 promoters. Plasmid pHPI-1748 was constructed by inserting the *PmeI*–*PmeI* fragment of pHPI-1706, containing the IRES-core/core+1(nt 9–825)–*myc* sequence in the presence of the N6 mutation, into the *SmaI* site of pBlue-script II KS (-) (Stratagene), under the control of the T7 promoter. Plasmid pHPI-1496 carries the *myc*-tagged HCV-1 core/core+1 sequence (nucleotide 515–825) of pHPI-1495, excised as a *PmeI* fragment and cloned into the *XbaI*-blunt-ended site of the pA-EUA2 expression vector. pA-EUA-2 was kindly provided by A. Epstein (University Claude Bernard, Lyon, France) [80]. Briefly, this plasmid carries two expression cassettes that are transcribed in opposite directions. The first comprises the herpes simplex virus type 1 immediate early 4 (IE4) ($\alpha 22/\alpha 47$) promoter controlling expression of the GFP protein, which permits the estimation of transfection efficiency. The second comprises the promoters HCMV and T7 followed by a pCI-derived chimeric intron that increases the level of gene expression, and a short polylinker (restriction sites *NheI*, *XbaI*, *NotI*). Plasmid pHPI-1579 was constructed following

Table 1. Summarized information concerning core+1 expression from the different constructs used in this study.

Plasmid (paternal vector)	Length of the HCV-1 sequence (nucleotides)	Mutation	Tag molecule	Primers	Forms of core+1 protein detected (GCA346 defined as codon 1 and frameshift site)	Elements mediating core+1 translation: start codons	Expected size (kDa)	Core coexpression
pHPI-1494 (pcDNA3.1(-)/Myc-His)	342–825	–	<i>myc</i>	C53, C203	not detectable in Huh-7	–	–	+
pHPI-1507 (pcDNA3.1(-)/Myc-His)	345–825	Deletion of core initiation codon	<i>myc</i>	N294, N295	core+1/S- <i>myc</i>	ATG core+1 85, 87 (internal initiation)	13	–
pHPI-1495 (pcDNA3.1(-)/Myc-His)	515–825	Deletion of core nts 342–514	<i>myc</i>		core+1/S- <i>myc</i>	ATG core+1 85, 87 (internal initiation)	13	–
pHPI-1705 (pcDNA3.1(-)/Myc-His)	9–825	–	<i>myc</i>		core+1/F- <i>myc</i> (detected in Çuh-7/Ö7)	ATG polyprotein (ribosomal frameshift)	22	+
pHPI-1706 (pcDNA3.1(-)/Myc-His)	9–825	–	<i>myc</i>		core+1/S- <i>myc</i>	ATG core+1 85, 87 (internal initiation)	13	–
pHPI-1509 (pcDNA3.1(-)/Myc-His)	342–825	N6 (CCG414 → TAA, Pro25 → stop in core ORF)	<i>myc</i>	N246, N247	core+1/S- <i>myc</i>	ATG core+1 85, 87 (internal initiation)	13	–
pHPI-1748 (pBluescript II KS-)	9–825	Deletion of 1 adenine (A) at core codons 8–11	<i>myc</i>		core+1/F- <i>myc</i>	ATG polyprotein/9As at codons 8–11 frameshift	22	+
pHPI-1496 (pA-EUA2)	515–825	Deletion of core nts 342–514	<i>myc</i>		core+1/S- <i>myc</i>	ATG core+1 85, 87 (internal initiation)	13	–
pHPI-1579 (pA-EUA2)	590–825	ATG core+1 85 with optimal context GCCCTCTATGG → CGGCCACCATGG	<i>myc</i>	N298, N300	core+1/S- <i>myc</i>	ATG core+1 85, 87 (internal initiation)	13	–
pHPI-1580 (pA-EUA2)	590–828	ATG core+1 85 with optimal context GCCCTCTATGG → CGGCCACCATGG	–	N298, N222	core+1/S	ATG core+1 85, 87	8.5	–

Table 2. List of priming oligonucleotides used in PCR. Restriction sites included in the primer sequence are underlined.

Primer name	Primer sequence	Primer pair	Annealing temp (°C)
C53 (sense)	GTGCTTGC <u>GAATTC</u> CCCCGGA	C53–C203	60
C203 (antisense)	CTC <u>GAATTC</u> AGTTGACGCCGTCTTCCAGAACC		
N294 (sense)	CGTAGACCGTGCACCAGCACGAATCCTAAAC	N294–N295	66
N295 (antisense)	GTTTAGGATTCGTGCTGGTGCACGGTCTACG		
N246 (sense)	CCTAAACCTCAAAAAAAAAACAACGTAACACC	N246–N247	59
N247 (antisense)	GGTGTACGTTTGTTTTTTTTTGAGGTTTAGG		
N298 (sense)	CCG <u>GAATTC</u> CGCCACCATGGCAATGAGGGCTCGGGTGGGCGGG	N298–N300	57
N300 (antisense)	G <u>GAATTC</u> CAGCGGTTTAAACTCAATG		
N222 (antisense)	CTC <u>GAATTC</u> AGTTCACGCCGTCTTCCAG	N298–N222	64
C54 (antisense)	CTC <u>GAATTC</u> ACTAGGTAGGCCGAAG	C53–C54	60

PCR amplification of the *myc*-tagged HCV-1 core/core + 1 sequence that is contained within nucleotides 590–825, using as template pHPI-1494 and the primer pair N298–N300 (Table 2). These primers introduced mutations in the context of the ATG85 initiator codon (nucleotide 598) of the core+1 ORF to convert it to an optimal Kozak context, CCGCCACCATGG [26]. Firstly, the N298–N300 PCR product was inserted into the *HincII* cloning site of pUC19 (BioLabs) in a 5' → 3' orientation to yield pHPI-1745. Subsequently, the *SmaI*–*PmeI* fragment of pHPI-1745, containing the core/ core+1(nt 590–825)–*myc* sequence, was cloned into the *XbaI*-blunt-ended site of pA-EUA2.

For the construction of pHPI-1580, the HCV-1 core/core + 1 sequence contained within nucleotides 590–828 (including the termination codon of the core+1 ORF), encoding the core + 1/S protein, was PCR amplified from pHPI-1494 using the primer pair N298–N222 (Table 2). Primer N298 introduces for ATG85 an optimal Kozak context, CCGCCACCATGG. The N298–N222 PCR fragment was digested with *EcoRI*, blunt-ended and inserted into the *XbaI*-blunt-ended site of pA-EUA2. Plasmid pHPI-1499 contains the HCV-1 core coding sequence (nucleotides 342–920). The core sequence was amplified using as template the plasmid pHPI-755 [16] and the primer pair C53–C54 (Table 2). The C53–C54 PCR product was digested with *EcoRI* and inserted into the *EcoRI* cloning site of pCI to yield pHPI-773. The *NheI*–*XbaI* fragment from pHPI-773, containing nucleotides 342–920 of the core sequence, was cloned into the *XbaI*-blunt-ended site of pA-EUA2 to produce pHPI-1499.

The plasmid pA-EUA2 + lacZ (kindly provided by A. Epstein, University Claude Bernard, Lyon, France) carries the coding sequence of β -gal, cloned into the pA-EUA2 vector. This plasmid will be referred to as the lacZ vector. For the construction of plasmid pHPI-1203, the HCV-1a (H) NS4B coding sequence (783 bp) obtained from plasmid p90-FL (kindly provided by C. Rice), preceded by a Met and an Ala codon, was inserted into the *EcoRI* and *Sall* cloning sites of pEGFP-N3.

For the PCR amplification of the core/core + 1 sequences, the following conditions were used: 94 °C for 5 min followed by 35 cycles of 94 °C for 1 min, annealing for 30 s, and 74 °C for 1 min, with a final extension at 74 °C for 10 min. For PCR site-directed mutagenesis the following conditions were used: 95 °C for 30 s followed by 18 cycles of 95 °C for 30 s, annealing for 1 min, and 68 °C for 10 min, with a final extension at 68 °C for 10 min.

Cells and transfection experiments

Huh-7/T7, a stable retrovirally transformed Huh-7 (human hepatoma) cell line that constitutively synthesizes the bacteriophage T7 RNA polymerase in the cytoplasm, was kindly provided by R. Bartenschlager (University of Heidelberg, Germany). Huh-7 and Huh-7/T7 cells were maintained in Dulbecco's modified Eagle's medium (Biochrom KG, Terre Haute, IN, USA), supplemented with 10% fetal bovine serum (Gibco, Rockville, MD), penicillin and streptomycin (100 U·mL⁻¹ and 100 μ g·mL⁻¹, respectively) and 2 mM L-glutamine. Specifically for Huh-7 cells, the culture medium was supplemented with non-essential amino acids (1 \times) (Biochrom KG), and for Huh-7/T7 cells with Zeocin (5 μ g·mL⁻¹) (Invitrogen). Cells seeded in six-well plates (Nunc, Naperville, IL), at a confluence of 60–70% for Huh-7 and 80–90% for Huh-7/T7 cells, were transfected using Lipofectamine Plus reagent (Invitrogen) according to the manufacturer's protocol. Cells were treated with the indicated proteasome inhibitors for 12 h before harvesting. Huh-7 cells were harvested at 48 h post transfection, whereas Huh-7/T7 cells at 24 h post transfection.

Immunoblotting

Cell monolayers were harvested 24 h post transfection and lysates were analyzed on a 13% SDS/PAGE gel as described previously [80].

Subcellular fractionation–phase separation of membrane proteins in Triton X-114 solution

Monolayers of Huh-7 cells, either transfected with plasmid vectors expressing core+1-*myc*, GFP or NS4B-GFP proteins, or left untransfected, were grown in six-well plates. Cell lysis and phase separation with Triton X-114 were performed as described previously [36]. After separation SDS/PAGE loading buffer was added to each sample and aliquots of the separated phases were analyzed on a 13% SDS/PAGE gel.

Preparation of nuclear and cytoplasmic extracts

Nuclear and cytoplasmic extracts from monolayers of Huh-7 cells either transfected with plasmid vectors expressing core+1-*myc* or GFP proteins, or from untransfected cells, were prepared by using the NE-PER[®] Nuclear and Cytoplasmic Extraction Reagents kit (Pierce, Rockford, IL) according to the manufacturer's instructions, in the presence of a protease inhibitor cocktail for mammalian extracts (Sigma).

Immunofluorescence microscopy

Huh-7 cells were prepared and incubated with the primary antibodies as previously described [80]. Following three washes with 0.05% w/v saponin in NaCl/P_i (NaCl/P_i-S), cells were further incubated for 1 h at room temperature with secondary anti-mouse and/or anti-rabbit sera conjugated to Alexa Fluor 546 or 647 (Molecular Probes, Eugene, OR) diluted 1 : 1000 in NaCl/P_i-S containing 2 mg·mL⁻¹ BSA. Following three washes with NaCl/P_i-S and three with NaCl/P_i, cells were finally mounted on glass slides (Super-Frost Plus; Menzel-Glaser, Braunschweig, Germany) with Mowiol (10% w/v Mowiol, 25% v/v glycerol, 100 mM HCl, pH 8.5) (Sigma). Images were acquired with the ×63 apochromat lens of a Leica TCS-SP1 four-channel confocal microscope equipped with argon ion laser and helium–neon laser.

Antibodies

For the production of the polyclonal antibody against the core+1 ORF, the peptide NK1, consisting of amino acids TYRSSAPLLEALPGP(C) (core+1 amino acids 135–149), was chemically synthesized, conjugated to keyhole limpet hemocyanin (KLH) and used to immunize rabbits using a classical protocol of immunization [81]. The antisera were collected 2 weeks after the last boost. The anti-(core+1) polyclonal serum was purified by a slightly modified affinity chromatography method based on CNBr-activated Sepharose 4B beads, as described previously [81]. The antibody was used in western blotting at a concentration of 1 µg·mL⁻¹ and in immunofluorescence analysis at

10 µg·mL⁻¹. The mouse mAb against core (amino acids 1–120) (Biogenesis, Brentwood, NH, USA) and against β-gal (Gibco) were used in western blotting at dilutions of 1 : 1000 and 1 : 500, respectively. The mouse anti-*myc* mAb (Invitrogen) was used in immunofluorescence analysis at a dilution of 1 : 100 and the rabbit polyclonal antibody against GFP (Santa Cruz Biotechnology, Santa Cruz, CA) was used in western blotting at a dilution of 1 : 100. The rabbit anti-(calnexin) polyclonal serum (Sigma) was used at a dilution of 1 : 250 and the mouse anti-(α-tubulin) mAb (Molecular Probes) and rabbit polyclonal (Invitrogen) antibodies were used at a dilution of 1 : 50 in immunofluorescence analysis. Mouse anti-(cyclin D1) mAb and the rabbit anti-actin polyclonal serum (Santa Cruz Biotechnology) were used in western blotting at dilutions of 1 : 500 and 1 : 200, respectively.

Acknowledgements

We are grateful to Dr R. Bartenschlager for kindly providing us with the Huh-7/T7 cell line. We also thank our colleagues from the Molecular Virology Laboratory for helpful discussions and Dr S. Khalili for the critical reading of the manuscript.

References

- Choo QL, Kuo G, Weiner AJ, Overby LR, Bradley DW & Houghton M (1989) Isolation of a cDNA clone derived from a blood-borne non-A, non-B viral hepatitis genome. *Science* **244**, 359–362.
- Di Bisceglie AM (2000) Natural history of hepatitis C: its impact on clinical management. *Hepatology* **31**, 1014–1018.
- Hoofnagle JH (2002) Course and outcome of hepatitis C. *Hepatology* **36**, S21–S29.
- Zoulim F, Chevallier M, Maynard M & Trepo C (2003) Clinical consequences of hepatitis C virus infection. *Rev Med Virol* **13**, 57–68.
- Houghton M & Abrignani S (2005) Prospects for a vaccine against the hepatitis C virus. *Nature* **436**, 961–966.
- Feld JJ & Hoofnagle JH (2005) Mechanism of action of interferon and ribavirin in treatment of hepatitis C. *Nature* **436**, 967–972.
- Murphy FA, Fauquet CM, Bishop DHL, Ghabrial SA, Jarvis AW, Martelli GP, Mayo MA & Summers MD (1995) *Virus Taxonomy. Sixth Report of the International Committee on Taxonomy of Viruses*. Springer-Verlag, Vienna.
- Reed KE & Rice CM (2000) Overview of hepatitis C virus genome structure, polyprotein processing, and protein properties. *Curr Top Microbiol Immunol* **242**, 55–84.
- Rice CM (2003) Hcv life cycle and targets for drug development. *Hepatitis Annual Update*, 123–142.

- 10 Penin F, Dubuisson J, Rey FA, Moradpour D & Pawlotsky JM (2004) Structural biology of hepatitis C virus. *Hepatology* **39**, 5–19.
- 11 Lindenbach BD & Rice CM (2005) Unravelling hepatitis C virus replication from genome to function. *Nature* **436**, 933–938.
- 12 Hellen CU & Pestova TV (1999) Translation of hepatitis C virus RNA. *J Viral Hepat* **6**, 79–87.
- 13 Rijnbrand RC & Lemon SM (2000) Internal ribosome entry site-mediated translation in hepatitis C virus replication. *Curr Top Microbiol Immunol* **242**, 85–116.
- 14 Walewski JL, Keller TR, Stump DD & Branch AD (2001) Evidence for a new hepatitis C virus antigen encoded in an overlapping reading frame. *RNA* **7**, 710–721.
- 15 Xu Z, Choi J, Yen TS, Lu W, Strohecker A, Govindarajan S, Chien D, Selby MJ & Ou J (2001) Synthesis of a novel hepatitis C virus protein by ribosomal frameshift. *EMBO J* **20**, 3840–3848.
- 16 Varaklioti A, Vassilaki N, Georgopoulou U & Mavromara P (2002) Alternate translation occurs within the core coding region of the hepatitis C viral genome. *J Biol Chem* **277**, 17713–17721.
- 17 Varaklioti R, Georgopoulou U, Vassilaki N & Mavromara P (2000) *Evidence for Alternate Translation within the Core Coding Region of the Hepatitis C Virus*. 7th International Meeting on Hepatitis C Virus and Related Viruses. Molecular Virology and Pathogenesis, Gold Coast, Australia.
- 18 Branch AD, Walewski JL, Gutierrez JA, Fernandez EJ, Im GY, Dieterich DT, Schiano TD, Sigal SH, Schilsky ML & Schwartz ME (2003) HCV alternate reading frame proteins (ARFPs) may be virulence factors that help the virus survive adverse conditions. *Hepatology* **38**, 468A–469A.
- 19 Komurian-Pradel F, Rajoharison A, Berland JL, Khouri V, Perret M, Van Roosmalen M, Pol S, Negro F & Paranhos-Baccala G (2004) Antigenic relevance of F protein in chronic hepatitis C virus infection. *Hepatology* **40**, 900–909.
- 20 Bain C, Parroche P, Lavergne JP, Duverger B, Vieux C, Dubois V, Komurian-Pradel F, Trepo C, Gebuhrer L, Paranhos-Baccala G, Penin F & Inchauspe G (2004) Memory T-cell-mediated immune responses specific to an alternative core protein in hepatitis C virus infection. *J Virol* **78**, 10460–10469.
- 21 Vassilaki N & Mavromara P (2003) Two alternative translation mechanisms are responsible for the expression of the HCV ARFP/F/core+1 coding open reading frame. *J Biol Chem* **278**, 40503–40513.
- 22 Baril M & Brakier-Gingras L (2005) Translation of the F protein of hepatitis C virus is initiated at a non-AUG codon in a +1 reading frame relative to the polyprotein. *Nucleic Acids Res* **33**, 1474–1486.
- 23 Roussel J, Pillez A, Montpellier C, Duverlie G, Cahour A, Dubuisson J & Wychowski C (2003) Characterization of the expression of the hepatitis C virus F protein. *J Gen Virol* **84**, 1751–1759.
- 24 Choi J, Xu Z & Ou JH (2003) Triple decoding of hepatitis C virus RNA by programmed translational frameshifting. *Mol Cell Biol* **23**, 1489–1497.
- 25 Xu Z, Choi J, Lu W & Ou JH (2003) Hepatitis C virus F protein is a short-lived protein associated with the endoplasmic reticulum. *J Virol* **77**, 1578–1583.
- 26 Kozak M (1987) At least six nucleotides preceding the AUG initiator codon enhance translation in mammalian cells. *J Mol Biol* **196**, 947–950.
- 27 Scherrer K, Imaizumi-Scherrer MT, Reynaud CA & Therwath A (1979) On pre-messenger RNA and transcriptions. A review. *Mol Biol Rep* **5**, 5–28.
- 28 Flint SJ (1981) Splicing and the regulation of viral gene expression. *Curr Top Microbiol Immunol* **93**, 47–79.
- 29 Boris-Lawrie K, Roberts TM & Hull S (2001) Retroviral RNA elements integrate components of post-transcriptional gene expression. *Life Sci* **69**, 2697–2709.
- 30 Zheng ZM & Baker CC (2006) Papillomavirus genome structure, expression, and post-transcriptional regulation. *Front Biosci* **11**, 2286–2302.
- 31 Goncalves MA & de Vries AA (2006) Adenovirus: from foe to friend. *Rev Med Virol* **16**, 167–186.
- 32 Hiscox JA (2003) The interaction of animal cytoplasmic RNA viruses with the nucleus to facilitate replication. *Virus Res* **95**, 13–22.
- 33 Gorlich D & Kutay U (1999) Transport between the cell nucleus and the cytoplasm. *Annu Rev Cell Dev Biol* **15**, 607–660.
- 34 Nachury MV & Weis K (1999) The direction of transport through the nuclear pore can be inverted. *Proc Natl Acad Sci USA* **96**, 9622–9627.
- 35 Lyman SK, Guan T, Bednenko J, Wodrich H & Gerace L (2002) Influence of cargo size on Ran and energy requirements for nuclear protein import. *J Cell Biol* **159**, 55–67.
- 36 Bordier C (1981) Phase separation of integral membrane proteins in Triton X-114 solution. *J Biol Chem* **256**, 1604–1607.
- 37 Branch AD, Stump DD, Gutierrez JA, Eng F & Walewski JL (2005) The hepatitis C virus alternate reading frame (ARF) and its family of novel products: the alternate reading frame protein/F-protein, the double-frameshift protein, and others. *Semin Liver Dis* **25**, 105–117.
- 38 Guruprasad K, Reddy BV & Pandit MW (1990) Correlation between stability of a protein and its dipeptide composition: a novel approach for predicting *in vivo* stability of a protein from its primary sequence. *Protein Eng* **4**, 155–161.

- 39 Hagglund R & Roizman B (2004) Role of ICP0 in the strategy of conquest of the host cell by herpes simplex virus 1. *J Virol* **78**, 2169–2178.
- 40 Huang J, Huang Q, Zhou X, Shen MM, Yen A, Yu SX, Dong G, Qu K, Huang P, Anderson EM *et al.* (2004) The poxvirus p28 virulence factor is an E3 ubiquitin ligase. *J Biol Chem* **279**, 54110–54116.
- 41 Mansouri M, Bartee E, Gouveia K, Hovey Nerenberg BT, Barrett J, Thomas L, Thomas G, McFadden G & Fruh K (2003) The PHD/LAP-domain protein M153R of myxomavirus is a ubiquitin ligase that induces the rapid internalization and lysosomal destruction of CD4. *J Virol* **77**, 1427–1440.
- 42 Coadou G, Gharbi-Benarous J, Megy S, Bertho G, Evrard-Todeschi N, Segeral E, Benarous R & Girault JP (2003) NMR studies of the phosphorylation motif of the HIV-1 protein Vpu bound to the F-box protein beta-TrCP. *Biochemistry* **42**, 14741–14751.
- 43 Kehn K, Fuente Cde L, Strouss K, Berro R, Jiang H, Brady J, Mahieux R, Pumfery A, Bottazzi ME & Kashanchi F (2005) The HTLV-I Tax oncoprotein targets the retinoblastoma protein for proteasomal degradation. *Oncogene* **24**, 525–540.
- 44 Thomas M, Pim D & Banks L (1999) The role of the E6–p53 interaction in the molecular pathogenesis of HPV. *Oncogene* **18**, 7690–7700.
- 45 Eom CY, Heo WD, Craske ML, Meyer T & Lehman IR (2004) The neural F-box protein NFB42 mediates the nuclear export of the herpes simplex virus type 1 replication initiator protein (UL9 protein) after viral infection. *Proc Natl Acad Sci USA* **101**, 4036–4040.
- 46 Twu JS & Schloemer RH (1987) Transcriptional *trans*-activating function of hepatitis B virus. *J Virol* **61**, 3448–3453.
- 47 Spandau DF & Lee CH (1988) *Trans*-activation of viral enhancers by the hepatitis B virus X protein. *J Virol* **62**, 427–434.
- 48 Yen TS (1996) Hepadnaviral X protein: review of recent progress. *J Biomed Sci* **3**, 20–30.
- 49 Choi BH, Park GT & Rho HM (1999) Interaction of hepatitis B viral X protein and CCAAT/enhancer-binding protein alpha synergistically activates the hepatitis B viral enhancer II/pregenomic promoter. *J Biol Chem* **274**, 2858–2865.
- 50 Kim JH, Kang S, Kim J & Ahn BY (2003) Hepatitis B virus core protein stimulates the proteasome-mediated degradation of viral X protein. *J Virol* **77**, 7166–7173.
- 51 Moriishi K, Okabayashi T, Nakai K, Moriya K, Koike K, Murata S, Chiba T, Tanaka K, Suzuki R, Suzuki T *et al.* (2003) Proteasome activator PA28gamma-dependent nuclear retention and degradation of hepatitis C virus core protein. *J Virol* **77**, 10237–10249.
- 52 Rullier A, Trimoulet P, Urbaniak R, Winnock M, Zauli D, Ballardini G, Rosenbaum J, Balabaud C, Bioulac-Sage P & Le Bail B (2001) Immunohistochemical detection of hcv in cirrhosis, dysplastic nodules, and hepatocellular carcinomas with parallel-tissue quantitative RT-PCR. *Mod Pathol* **14**, 496–505.
- 53 Ruster B, Zeuzem S & Roth WK (1996) Hepatitis C virus sequences encoding truncated core proteins detected in a hepatocellular carcinoma. *Biochem Biophys Res Commun* **219**, 911–915.
- 54 Yeh CT, Lu SC, Chu CM & Liaw YF (1997) Molecular cloning of a defective hepatitis C virus genome from the ascitic fluid of a patient with hepatocellular carcinoma. *J Gen Virol* **78**, 2761–2770.
- 55 Yeh CT, Lo SY, Dai DI, Tang JH, Chu CM & Liaw YF (2000) Amino acid substitutions in codons 9–11 of hepatitis C virus core protein lead to the synthesis of a short core protein product. *J Gastroenterol Hepatol* **15**, 182–191.
- 56 Hayashi J, Furusyo N, Ariyama I, Sawayama Y, Etoh Y & Kashiwagi S (2000) A relationship between the evolution of hepatitis C virus variants, liver damage, and hepatocellular carcinoma in patients with hepatitis C viremia. *J Infect Dis* **181**, 1523–1527.
- 57 Ruster B, Zeuzem S, Krump-Konvalinkova V, Berg T, Jonas S, Severin K & Roth WK (2001) Comparative sequence analysis of the core- and NS5-region of hepatitis C virus from tumor and adjacent non-tumor tissue. *J Med Virol* **63**, 128–134.
- 58 Alam SS, Nakamura T, Naganuma A, Nozaki A, Nouse K, Shimomura H & Kato N (2002) Hepatitis C virus quasispecies in cancerous and noncancerous hepatic lesions: the core protein-encoding region. *Acta Med Okayama* **56**, 141–147.
- 59 Ogata S, Nagano-Fujii M, Ku Y, Yoon S & Hotta H (2002) Comparative sequence analysis of the core protein and its frameshift product, the F protein, of hepatitis C virus subtype 1b strains obtained from patients with and without hepatocellular carcinoma. *J Clin Microbiol* **40**, 3625–3630.
- 60 Miladi A, Lavergne J, Hezode C, Dhumeaux D, Penin F & MPJ (2004) *Prevalence of Anti-HCV F (Frameshift) Protein Antibodies in Patients with Various Forms of HCV Infection and the Putative Physiological Role of F Protein*. 11th International Symposium on Hepatitis C Virus and Related Viruses, 3–7 October, Heidelberg, Germany.
- 61 Tusnady GE & Simon I (1998) Principles governing amino acid composition of integral membrane proteins: application to topology prediction. *J Mol Biol* **283**, 489–506.
- 62 Tusnady GE & Simon I (2001) The HMMTOP transmembrane topology prediction server. *Bioinformatics* **17**, 849–850.
- 63 Egger D, Wolk B, Gosert R, Bianchi L, Blum HE, Moradpour D & Bienz K (2002) Expression of hepatitis

- C virus proteins induces distinct membrane alterations including a candidate viral replication complex. *J Virol* **76**, 5974–5984.
- 64 Mottola G, Cardinali G, Ceccacci A, Trozzi C, Bartholomew L, Torrisi MR, Pedrazzini E, Bonatti S & Migliaccio G (2002) Hepatitis C virus nonstructural proteins are localized in a modified endoplasmic reticulum of cells expressing viral subgenomic replicons. *Virology* **293**, 31–43.
- 65 Gosert R, Egger D, Lohmann V, Bartenschlager R, Blum HE, Bienz K & Moradpour D (2003) Identification of the hepatitis C virus RNA replication complex in Huh-7 cells harboring subgenomic replicons. *J Virol* **77**, 5487–5492.
- 66 Walewski JL, Gutierrez JA, Branch-Elliman W, Stump DD, Keller TR, Rodriguez A, Benson G & Branch AD (2002) Mutation master: profiles of substitutions in hepatitis C virus RNA of the core, alternate reading frame, and NS2 coding regions. *RNA* **8**, 557–571.
- 67 Sander C & Schneider R (1991) Database of homology-derived protein structures and the structural meaning of sequence alignment. *Proteins* **9**, 56–68.
- 68 Efferth T (2003) Adenosine triphosphate-binding cassette transporter genes in ageing and age-related diseases. *Ageing Res Rev* **2**, 11–24.
- 69 Kapadia SB & Chisari FV (2005) Hepatitis C virus RNA replication is regulated by host geranylgeranylation and fatty acids. *Proc Natl Acad Sci USA* **102**, 2561–2566.
- 70 Gao L, Tu H, Shi ST, Lee KJ, Asanaka M, Hwang SB & Lai MM (2003) Interaction with a ubiquitin-like protein enhances the ubiquitination and degradation of hepatitis C virus RNA-dependent RNA polymerase. *J Virol* **77**, 4149–4159.
- 71 Pavio N, Taylor DR & Lai MM (2002) Detection of a novel unglycosylated form of hepatitis C virus E2 envelope protein that is located in the cytosol and interacts with PKR. *J Virol* **76**, 1265–1272.
- 72 Franck N, Le Seyec J, Guguen-Guillouzo C & Erdtmann L (2005) Hepatitis C virus NS2 protein is phosphorylated by the protein kinase CK2 and targeted for degradation to the proteasome. *J Virol* **79**, 2700–2708.
- 73 Fujita M, Akari H, Sakurai A, Yoshida A, Chiba T, Tanaka K, Strebel K & Adachi A (2004) Expression of HIV-1 accessory protein Vif is controlled uniquely to be low and optimal by proteasome degradation. *Microbes Infect* **6**, 791–798.
- 74 Reichel C & Beachy RN (2000) Degradation of tobacco mosaic virus movement protein by the 26S proteasome. *J Virol* **74**, 3330–3337.
- 75 Drugeon G & Jupin I (2002) Stability *in vitro* of the 69K movement protein of turnip yellow mosaic virus is regulated by the ubiquitin-mediated proteasome pathway. *J Gen Virol* **83**, 3187–3197.
- 76 Rummenapf T, Stark R, Heimann M & Thiel HJ (1998) N-Terminal protease of pestiviruses: identification of putative catalytic residues by site-directed mutagenesis. *J Virol* **72**, 2544–2547.
- 77 Strebel K & Beck E (1986) A second protease of foot-and-mouth disease virus. *J Virol* **58**, 893–899.
- 78 Yamasaki K, Wehl CC & Roos RP (1999) Alternative translation initiation of Theiler's murine encephalomyelitis virus. *J Virol* **73**, 8519–8526.
- 79 Sambrook J, Fritsch EF & Maniatis T (1989) *Molecular Cloning: A Laboratory Manual*. Cold Spring Harbor Laboratory Press, Cold Spring Harbor, NY.
- 80 Kalamvoki M & Mavromara P (2004) Calcium-dependent calpain proteases are implicated in processing of the hepatitis C virus NS5A protein. *J Virol* **78**, 11865–11878.
- 81 Harlow E & Lane D (1988) *Antibodies. A Laboratory Manual*. Cold Spring Harbor Laboratory Press, Cold Spring Harbor, NY.